Modulated coherent Raman beats

E. W. Van Stryland
Physics Department, North Texas State University, Denton, Texas 76203

R. L. Shoemaker
Optical Sciences Center, University of Arizona, Tucson, Arizona 85721

(Received 16 April 1979)

The authors study the phenomenon of coherent Raman beats in $^{15}NH_3$ using a CO_2 laser and Stark switching. In particular, a three-level system in which the two upper levels always remain split by a few MHz is prepared by switching the transitions into resonance with a short Stark pulse whose bandwidth is large enough to coherently excite both transitions. When one of the coherently excited levels remains in resonance with the laser after the Stark pulse, this system exhibits a qualitatively new effect which has not been seen heretofore. For Stark shifts on the order of the upper-state splitting or smaller, the Raman beat is amplitude modulated at a frequency related to the optical nutation frequency. This is interpreted as being due to an interaction between the two-photon coherent Raman beat process and a single-photon optical nutation process which occurs simultaneously. Numerical calculations as well as a simple analytic model are presented to support this interpretation. By reducing the laser power, one can make the modulation of the Raman beat disappear. From the Raman signal in this regime the permanent electric dipole moment of $^{15}NH_3$ in an excited vibrational state is determined and the Raman beat decay rate measured. By comparing the latter result with a delayed optical nutation measurement we show that phase-changing collisions are negligible for the transition studied.

I. INTRODUCTION

In 1972, Shoemaker and Brewer reported the observation of a two-photon coherent transient effect which is now known as coherent Raman beats.[1] The phenomenon arose when a coherently excited three-level (or multi-level) system was driven slightly off resonance by a laser field. Very strong coherent Raman transitions can occur in this situation and appear at a detector placed in the laser beam as a long-lived heterodyne beat signal between the laser field and the radiation emitted during the Raman scattering process. Note that the forward scattered Raman field amplitude is observed in this case rather than the off-axis Raman scattered intensity that is monitored in ordinary Raman experiments. This unusual effect, which is closely related to two-photon free induction decay,[2-4] has aroused considerable theoretical attention[5-8] and has also been used to measure collisional decay rates.[9]

In earlier experiments, coherent preparation of the system was achieved by resonantly exciting a transition having several degenerate levels.[1,9] A Stark field was then suddenly applied which split the degenerate levels, allowing Raman transitions between the split levels to occur and produce the Raman beat signal. In this paper we report an extension of the coherent Raman beat phenomena to a somewhat different type of transition in which no level degeneracy effects are present. Specifically, we examine a three-level system in which two upper levels always remain split by a few MHz and have allowed transitions to a single common lower level whose energy can be varied by means of a Stark field (see Fig. 1). Coherent preparation is achieved by applying a Stark pulse short enough (i.e., bandwidth wide enough) to simultaneously excite both transitions. In this situation we find that the Raman transitions giving rise to the coherent Raman beat signal can become resonant and produce a new effect which involves the interaction of the two-photon Raman process with the single-photon process of optical nutation (Rabi flopping). This occurs when one of the level pairs remains in one-photon resonance after the Stark pulse. A detailed discussion of this interaction, which ap-

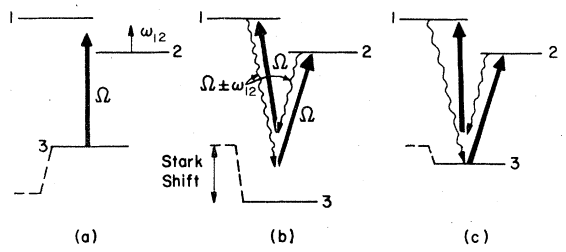

FIG. 1. Coherent Raman beats. (a) A short Stark pulse shifts level 3 so that the laser field of frequency Ω can excite a coherent superposition of levels 1 and 2. (b) At the end of the pulse, level 3 is shifted out of resonance and Raman transitions take place as shown with radiation being emitted at $\Omega \pm \omega_{12}$. (c) If a smaller Stark shift is used, one of the Raman processes can become resonant, allowing optical nutation and Raman transitions to occur simultaneously.

pears as an amplitude modulation of the coherent Raman beat signal, is given in Sec. II below. In addition, by changing the experimental conditions, the amplitude modulation could be made to disappear, and this regime was used to make measurements of the $^{15}NH_3$ molecular dipole moment in an excited vibrational state and of the Raman beat decay time. These results and their implications are also discussed.

Our experiments were performed using the $(\nu_2,J,K)=(0^a,2,2)\rightarrow(1^s,3,2)$ transition in $^{15}NH_3$ which lies 360 MHz above the $R(40)$ CO_2 laser line at 10.125 μm.[10] Transitions arising from the $M_J=\pm2$ component of the lower level can be shifted into resonance with the CO_2 laser using a dc bias field of ~6000 V/cm. With the CO_2 laser radiation polarized perpendicular to the bias field, $\Delta M_J=\pm1$ selection rules are obtained so that only the $M_J=\pm2\rightarrow\pm3$ and $\pm2\rightarrow\pm1$ components of the transition are excited. Thus we have a simple three-level system of the type shown schematically in Fig. 1(a). The splitting between the two upper states $M_J=\pm1$ and $M_J=\pm3$ (the levels labeled 1 and 2 in the figure) is only 5.27 MHz, much less than the 80-MHz Doppler width.

A 1.5-m grating controlled, stable cw CO_2 laser of the type described by Freed is used in the experiment.[11] It has an output power of about 0.5 W TEM_{00} on the 10-μm $R(40)$ line that was used. The laser beam passes through a sample cell containing a pair of 4.5 cm×30 cm stainless-steel Stark plates. These plates are precision lapped to a flatness of better than 0.0003 cm and are separated by a set of six 0.4445 ±0.0005 cm fused quartz spacers, thus producing very uniform electric fields. The sample cell is filled with $^{15}NH_3$ (ProChem 99 at.% ^{15}N) to a pressure between 0 and 10 mTorr as determined by a CGS Barocel capacitance manometer. After passing through the cell, the laser beam strikes an Au:Ge detector whose output is amplified by a wideband (20 KHz to 8 MHz) preamp and then sent to either an oscilloscope or a PAR 162 boxcar integrator and X-Y plotter for display.

To perform a Raman beat experiment, a voltage pulse (typically 135 V/cm and 0.1 μsec long) is applied across the Stark plates in addition to the dc bias field. For simplicity, consider first the case where no modulation of the Raman beat is observed. At the time the pulse is turned on, the lower level is shifted several MHz causing two distinct effects to occur simultaneously. First, velocity groups of molecules which were in resonance with the laser are briefly shifted out of resonance and then back into resonance at the end of the pulse. This produces an optical nutation signal which merely forms a background on which the coherent Raman beat signal is superimposed. Second, other molecular velocities are shifted *into* resonance during the pulse and excited by the laser. The pulse length determines the velocity bandwidth of molecules thus excited, and, if the length is sufficiently short, will allow some molecules to be excited to a coherent superposition of both excited states [see Fig. 1(a)]. At the end of the pulse, these excited molecules are shifted out of resonance so that they now see an off-resonant driving field. This field induces near-resonant Raman (two-photon) transitions between levels 1 and 2 as shown in Fig. 1(b). As can be seen from the figure, conservation of energy requires that the radiation emitted in the Raman process have frequency $\Omega+\omega_{12}$ or $\Omega-\omega_{12}$. Furthermore, because the superposition of excited states was initially prepared using a coherent laser field propagating in the z direction, the forward scattered Raman emission induced by that field after the Stark voltage pulse is also coherent, i.e., emission in the z direction at $\Omega\pm\omega_{12}$ by any given molecule is in phase with the emission of all other emitting molecules. Hence a detector placed in the laser beam behind the cell will see coherent fields at $\Omega\pm\omega_{12}$ in addition to the laser field, resulting in a heterodyne beat signal of frequency ω_{12} between the laser and the emission. The molecules excited by the pulse will also produce optical free-induction decay signals, but these signals quickly decay to zero in a time less than or equal to the excitation pulse length and will be ignored.[12] Figure 2 shows an example of a Raman beat signal in $^{15}NH_3$ when a low laser intensity is used. The high-frequency oscillation (~5 MHz) is the Raman beat signal and is similar to previous Raman beat observations in $^{13}CH_3F$, where degenerate levels were excited.[1]

Note that Doppler effects due to molecular motion do not affect the Raman beat (to first order, at least) because a molecule moving with velocity component v_z sees the laser frequency Doppler downshifted to $\Omega'=\Omega-k_Lv_z$ and hence emits at $\Omega'\pm\omega_{12}$. In the laboratory frame $+z$ direction, however, this emission appears as a Doppler upshifted frequency $(\Omega'\pm\omega_{12})+kv_z\simeq\Omega\pm\omega_{12}$ since $k\simeq k_L$. Thus, the emitted frequency is independent of molecular velocity and there is no Doppler dephasing as in the single-photon process of optical free induction decay. As a result, the coherent Raman beat signal is quite long lived and its decay is determined only by the collisional decay of the off-diagonal density matrix element ρ_{12}.

In the above discussion, we have assumed that the velocity groups of molecules which are excited during the initial Stark voltage pulse are shifted sufficiently far from resonance after the pulse that

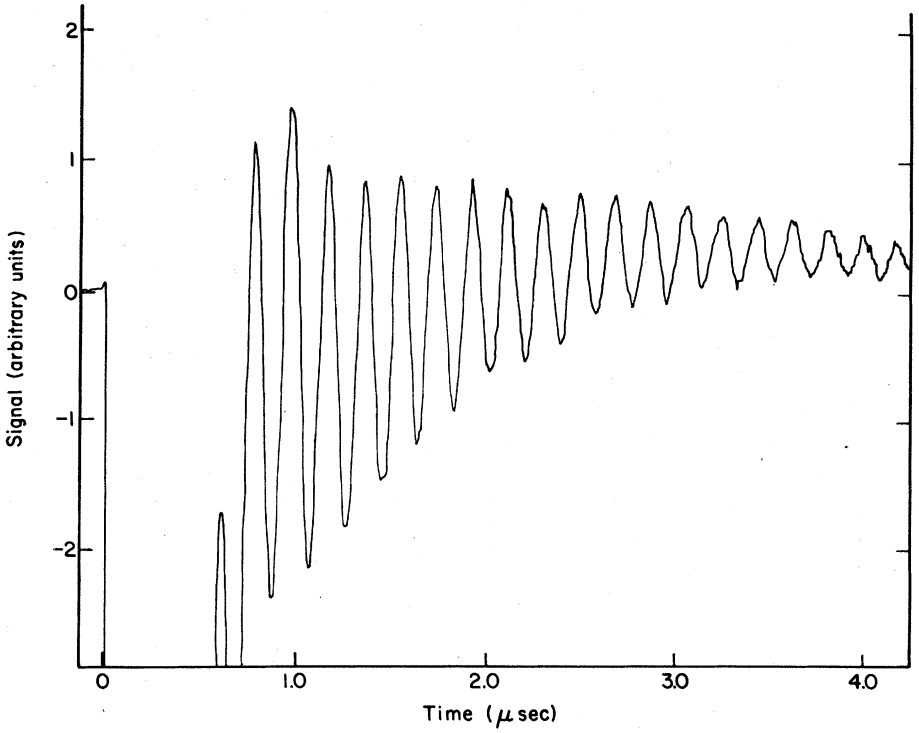

FIG. 2. Raman beats in $^{15}NH_3$ using a low intensity CO_2 beam. The high-frequency oscillation (~5 MHz) is the Raman beat signal.

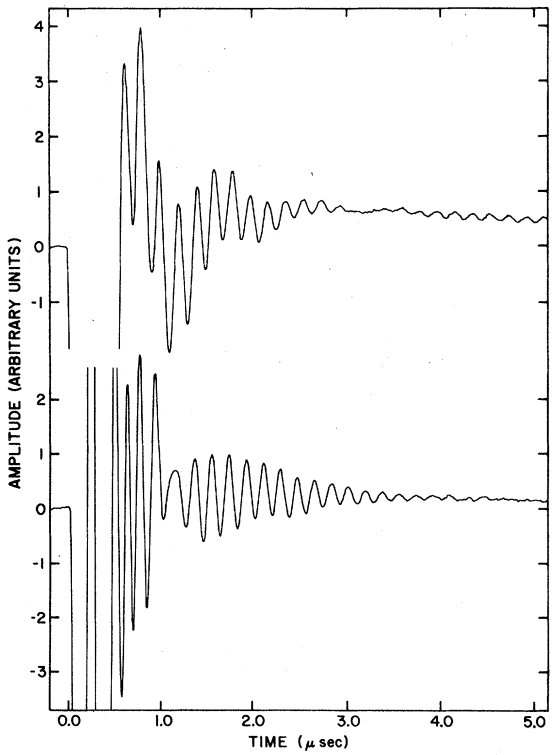

FIG. 3. Modulated Raman beat signals in $^{15}NH_3$ for two CO_2 laser intensities. In the upper trace a minimum in the Raman beat appears at ~3 μsec. In the lower trace a higher laser power was used and the minimum has moved in to ~ 1 μsec.

only the Raman transitions have an appreciable probability of occurring. The molecules are not excited further via single-photon transitions. Looking at the energy-level diagram of Fig. 1, however, it is clear that a lower voltage Stark pulse can be used to cause a smaller frequency shift (on the order of half the level splitting ω_{12}) such that some of the molecules excited to a superposition of levels 1 and 2 during the pulse now have the $3 \rightarrow 1$ or $3 \rightarrow 2$ transition resonant *after* the pulse. This situation is shown in Fig. 1(c). Here two processes occur simultaneously. First, Raman transitions will occur as before, with the $2 \rightarrow 1$ transition being especially intense because it is a resonant Raman process. In addition, the fact that the laser field is resonant with the $3 \rightarrow 2$ transition will cause population to be driven back and forth between these levels (optical nutation).[13] The Raman and optical nutation processes must clearly interact with each other because both are acting on the same molecules. While this interaction can be quite complicated in general, the situation simplifies if the optical nutation frequency $\wp_{ab}E_0/\hbar$ is much less than the level splitting ω_{12}. In this case, the interaction appears primarily as an amplitude modulation of the Raman beat as shown in Fig. 3. In Sec. II below, we give a quantitative discussion of how this occurs.

II. THEORY

In an earlier theoretical treatment of coherent Raman beats, Brewer and Hahn utilized a pertur-

bation theory treatment of the density matrix equations to calculate the Raman beat.[6] In a later paper Brewer and Hahn[7] solve these equations exactly during the preparative stage but are again forced to use perturbation theory to describe the transient decay. Unfortunately, this treatment cannot be used to analyze our experiments because the amplitude modulation of the Raman beat involves optical nutation and this is a strong-field, nonlinear process which cannot be described by perturbation theory. We should note, however, that the Brewer-Hahn treatment does predict an intensity dependent decay of the Raman beat. This effect may be thought of as a weak-field precursor to the strong-field effects being considered in this paper.

Since a nonperturbative solution to the density-matrix equations of motion for a three-level system is what really is required here, one is forced to resort to numerical methods. Even this is no small task, however, since a set of six simultaneous differential equations must be solved at each point in time to obtain the response of just one velocity group of molecules. This process must then be repeated for every molecular velocity within the Doppler line, followed by a numerical integration of the solutions over all velocities at each point in time one wishes to consider. A considerable simplification can be obtained, however, if one is willing to ignore some of the nonessential physics in the problem. In particular, we note that decay processes and processes which pump new molecules into the three levels do not affect the Raman beat signal in any fundamental way.[6] If we drop these terms from the density-matrix equations of motion, the resulting equations are equivalent to a much simpler set of three differential equations for the probability amplitudes of being in levels 1, 2, or 3. The characteristic cubic equation associated with this set of equations is readily solved by computer and the complete solution for the probability amplitudes can then be written down analytically in terms of the roots of the cubic.[14] This wave equation approach is far simpler than the alternative of numerically integrating the density-matrix equations. Sargent and Horwitz[15] solved the wave equation exactly for the case where the laser frequency lies halfway between the upper two levels in Fig. 1. Schenzle and Brewer[16] solve Schrödinger's equation for several special cases but not the particular case where one level is in single-photon resonance with the laser excitation. They note that this case must be solved numerically.

An additional advantage of working with the probability amplitudes is that a simple approximate solution for the modulated Raman beat problem can be found which gives some insight into the nature of the processes which are occuring. This solution is presented below following a brief presentation of the basic theoretical equations.

To develop a quantitative theory for the modulated Raman beat, we begin by taking the optical field to be a linearly polarized plane wave

$$E_L = \hat{x}[E_0 \cos(\Omega t - kz)] . \tag{1}$$

In the dipole approximation, the Hamiltonian in the presence of this field is

$$\mathcal{H} = \mathcal{H}_0 - E_0 \cos(\Omega' t - kz') \sum_i e_i x_i , \tag{2}$$

where x_i is the x coordinate of the ith electron or nucleus in the molecule with respect to the center of mass and the summation on i is over all charges e_i in the molecule. Also, E_L has been transformed into the rest-frame coordinate system of a molecule having a component of velocity v_z. In this frame, the frequency is Doppler shifted to $\Omega' = \Omega - kv_z$ and $z' = z - v_z t$ is the new z coordinate of the molecular center of mass. We assume an optically thin sample so that E_0 is independent of z'. This condition is well satisfied in our experiments where the peak absorption is <1%.

The wave function for a molecule in the presence of the optical field may be expanded in terms of the field-free eigenfunctions ψ_n as

$$\Psi = \sum_n c_n(t) \psi_n . \tag{3}$$

This relation together with the Schrödinger equation yields an equation of motion for the probability amplitudes c_n,

$$i\hbar \dot{c}_n = \hbar W_n c_n - E_0 \cos(\Omega' t - kz') \sum_j \wp_{nj} c_j , \tag{4}$$

where $\hbar W_n$ is the energy of level n and $\wp_{nj}$ is the x component of the transition dipole matrix element between levels n and j. We assume the phases of the field-free eigenfunctions have been chosen such that the $\wp_{nj}$'s are real.

Since we are interested in the three-level system shown in Fig. 1, we need to consider only the probability amplitude equations for c_1, c_2, and c_3. Using the definitions

$$\begin{aligned} c_1 &\equiv \tilde{c}_1 \exp[-i(\Omega' t - kz')] , \\ c_2 &\equiv \tilde{c}_2 \exp[-i(\Omega' t - kz')] , \end{aligned} \tag{5}$$

setting the zero of energy to be the lower level ($\hbar W_3 = 0$), and making the rotating wave approximation, we have

$$\begin{aligned} &\dot{\tilde{c}}_1 = i\delta_1 \tilde{c}_1 + i\alpha_{13} c_3 , \quad \dot{\tilde{c}}_2 = i\delta_2 \tilde{c}_2 + i\alpha_{23} c_3 , \\ &\dot{c}_3 = i\alpha_{13} \tilde{c}_1 + i\alpha_{23} \tilde{c}_2 . \end{aligned} \tag{6}$$

Here $\alpha_{13}=\wp_{13}E_0/2\hbar$, $\alpha_{23}=\wp_{23}E_0/2\hbar$, and $\delta_1=\Omega'-\omega_{13}$, $\delta_2=\Omega'-\omega_{23}$, where $\omega_{ij}=W_i-W_j$. Equation (6) must be solved for two distinct time periods. We start in thermal equilibrium at time $-t_{ex}$ with $c_3(-t_{ex})=1$, $c_1(-t_{ex})=c_2(-t_{ex})=0$ and must solve the equations for an excitation pulse of duration t_{ex}. We then know $c_1(0)$, $c_2(0)$, $c_3(0)$; the values of the c_i's at the end of the excitation pulse ($t=0$). These values form the initial conditions for the calculation of the Raman beat during the period $t>0$. Equation (6) is a set of linear differential equations with constant coefficients and hence is readily solved by standard methods, with the solutions being expressed in terms of the roots of a characteristic cubic equation,

$$\lambda^3-(\delta_1+\delta_2)\lambda^2+[\delta_1\delta_2-(\alpha_{13}^2+\alpha_{23}^2)]\lambda+\alpha_{13}^2\delta_2+\alpha_{23}^2\delta_1=0\,. \tag{7}$$

Unless some approximation can be made, however, this cubic must be solved by numerical methods in order to obtain usable results.

Once either a numerical or analytic solution for the c_i's is obtained, the expectation value of the dipole moment for any molecule can be calculated from

$$\langle\mu\rangle=\wp_{13}(c_1c_3^*+c_1^*c_3)+\wp_{23}(c_2c_3^*+c_2^*c_3)\,. \tag{8}$$

This expression is more conveniently written in terms of $\tilde{c}_1$ and $\tilde{c}_2$ as

$$\langle\mu\rangle=\mu_c\cos(\Omega t-kz)+\mu_s\sin(\Omega t-kz)\,, \tag{9}$$

where

$$\mu_c=\wp_{13}\tilde{c}_1c_3^*+\wp_{23}\tilde{c}_2c_3^*+\text{c.c.}$$

$$\mu_s=-i\wp_{13}\tilde{c}_1c_3^*-i\wp_{23}\tilde{c}_2c_3^*+\text{c.c.}$$

The macroscopic polarization induced in the sample is then obtained by summing over all molecules, i.e.,

$$\begin{aligned}P(z,t)&=\left(\int_{-\infty}^{\infty}\mu_cN(v_z)\,dv_z\right)\cos(\Omega t-kz)\\&\quad+\left(\int_{-\infty}^{\infty}\mu_sN(v_z)\,dv_z\right)\sin(\Omega t-kz)\\&\equiv P_c(t)\cos(\Omega t-kz)+P_s(t)\sin(\Omega t-kz)\,,\end{aligned} \tag{10}$$

where $N(v_z)=(N/\bar{u}\sqrt{\pi})\exp(-v_z^2/\bar{u}^2)$ is the number density of molecules with velocity v_z, and $\bar{u}=(2k_BT/m)^{1/2}$ is the most probable molecular speed.

In the simple case where the sample is short and optically thin, one can readily show that the amount of radiation absorbed or emitted by the sample is just proportional to P_s.[12] The relation is

$$I(t)=I_0-\tfrac{1}{2}\Omega LE_0P_s(t)\,, \tag{11}$$

where I_0 is the incident intensity, L is the length of the sample, and $I(t)$ is the intensity of the radiation field after passing through the sample. $I(t)$ is exactly the quantity that one measures in a Raman beat experiment since the detector is placed directly in the laser beam behind the sample. Combining Eqs. (9)–(11), we have

$$I(t)=I_0-2\hbar\Omega L\int_{-\infty}^{\infty}N(v_z)[\alpha_{13}\,\mathrm{Im}(\tilde{c}_1c_3^*)+\alpha_{23}\,\mathrm{Im}(\tilde{c}_2c_3^*)]\,dv_z \tag{12}$$

as the expression for the observed signal in terms of the c_i's.

At the end of this section we discuss the results of numerical calculations using Eqs. (6) and (12). Before doing this, however, it may be useful to develop an approximate analytic model which exhibits many of the primary features of the experiments.

The key to an analytical treatment can be found by looking again at Fig. 1. As was pointed out in the introduction, amplitude modulation of the Raman beat is expected to appear when molecules excited to a superposition of levels 1 and 2 during an excitation pulse are shifted into resonance with the $3\rightarrow2$ transition after the pulse. As can be seen from Fig. 1(c), these molecules are detuned from the $3\rightarrow1$ transition by an amount $\delta_1\simeq\omega_{12}$ after the pulse. Furthermore, the level splitting ω_{12} is much greater than the Rabi-flopping frequencies $2\alpha_{13}$ and $2\alpha_{23}$ in our experiments. Thus the inequality $\delta_1\gg\alpha_{13}$ should be valid for the molecules of interest after the laser pulse. Looking now at Eq. (6) we see that this inequality allows one to obtain an approximate solution. Specifically, we neglect the second term in the $\dot{\tilde{c}}_1$ equation compared to the first to obtain

$$\dot{\tilde{c}}_1=i\delta_1\tilde{c}_1\,, \tag{13}$$

which has the trivial solution

$$\tilde{c}_1(t)=\tilde{c}_1(0)\exp(i\delta_1t)\,. \tag{14}$$

Here $\tilde{c}_1(0)$ is the value of $\tilde{c}_1$ at the end of the excitation pulse. The solution for $\tilde{c}_1$ may now be substituted into the $\dot{\tilde{c}}_2$ and $\dot{c}_3$ equations [see Eq. (6)] to obtain solutions for both c_3 and $\tilde{c}_2$. Since we have assumed δ_1, $\omega_{12}\gg\alpha_{13}$, α_{23} for the molecules of interest, we may also neglect terms of order α_{13}/δ_1, etc. compared to unity in these solutions to obtain

$$\begin{aligned}\tilde{c}_2(t)&=\tilde{c}_2(0)\exp(\tfrac{1}{2}i\delta_2t)\cos(\tfrac{1}{2}gt)+i[\delta_2\tilde{c}_2(0)+2\alpha_{23}c_3(0)]\exp(\tfrac{1}{2}i\delta_2t)\sin(\tfrac{1}{2}gt)/g\,,\\c_3^*(t)&=c_3^*(0)\exp(-\tfrac{1}{2}i\delta_2t)\cos(\tfrac{1}{2}gt)-i[2\alpha_{23}\tilde{c}_2^*(0)-\delta_2c_3^*(0)]\exp(-\tfrac{1}{2}i\delta_2t)\sin(\tfrac{1}{2}gt)/g\,,\end{aligned} \tag{15}$$

as our approximate solutions for $\tilde{c}_2$ and c_3^* after the excitation pulse. Here $g=(\delta_2^2+4\alpha_{23}^2)^{1/2}$. We now want to calculate the Raman beat signal using Eq. (12). To do this, note first of all that $I_0-I(t)$ is the net absorption or emission due to all transient effects occurring in the sample, not just the Raman beat. The contributions from the various effects can readily be separated out by making use of the fact that each coherent transient effect has its own characteristic oscillation frequency and dependence on initial conditions. For example, all the terms arising from $\mathrm{Im}(\tilde{c}_2 c_3^*)$ oscillate only at $\sin(gt)$ or $\cos(gt)$ and hence are optical nutation signals arising from single-photon transitions between levels 2 and 3. The three terms arising from $\mathrm{Im}(\tilde{c}_1 c_3^*)$ have more complex oscillation frequencies, and, in particular, they all have frequency components at ω_{12} since $\frac{1}{2}\delta_2-\delta_1=\omega_{12}-\frac{1}{2}\delta_2$. An oscillation at ω_{12} is characteristic of the Raman beat. However, in the case at hand, optical free induction decay signals from the $1\rightarrow 3$ transition will also occur at this frequency since we have assumed that the laser is detuned from the $1\rightarrow 3$ transition by ω_{12}, i.e., we assumed it was resonant with the $2\rightarrow 3$ transition. To see which terms contain the Raman beat, we must examine their dependence on initial conditions. The amplitude of two of the terms depends on $\tilde{c}_1(0)c_3^*(0)$, while the remaining term depends on $\tilde{c}_1(0)\tilde{c}_2^*(0)$. Since the Raman beat is a two-photon effect which requires a coherent superposition of levels 1 and 2 to occur, only the $\tilde{c}_1(0)c_2^*(0)$ term contains the Raman beat.[6] The other two terms depend only on having a coherent superposition of levels 1 and 3 which is characteristic of optical free induction decay.[17] Thus the coherent Raman beat signal is

given by

$$I_R(t)=I_0-2\alpha_{13}\hbar\Omega L\int_{-\infty}^{\infty}N(v_z)\,\mathrm{Im}\left\{-2i\alpha_{23}\tilde{c}_1(0)\tilde{c}_2^*(0)\exp\left[i\left(\delta_1-\frac{\delta_2}{2}\right)t\right]\frac{1}{g}\sin\left(\tfrac{1}{2}gt\right)\right\}dv_z\,. \tag{16}$$

On taking the imaginary part of the expression in curly brackets and separating out the $\omega_{12}t$ dependence, four terms are obtained. Two of these terms are odd functions of v_z, however, and may be dropped since they will give zero when the Doppler integration is performed. After some rearrangement, we then find

$$I_R(t)=I_0+4\hbar\alpha_{13}\alpha_{23}\Omega L\int_{-\infty}^{\infty}N(v_z)\left|\tilde{c}_1(0)\tilde{c}_2^*(0)\right|^2\frac{1}{g}\sin\left(\frac{gt}{2}\right)\cos\left(\frac{\delta_2 t}{2}\right)\cos(\omega_{12}t+\phi)\,dv_z\,, \tag{17}$$

where

$$\phi=\tan^{-1}\{\mathrm{Im}[\tilde{c}_1(0)\tilde{c}_2^*(0)]/\mathrm{Re}[\tilde{c}_1(0)\tilde{c}_2^*(0)]\}.$$

This is as far as we can carry the problem because the Doppler integral cannot be done analytically. Furthermore, we have not calculated values for $|\tilde{c}_1(0)\tilde{c}_2^*(0)|^2$, which depend strongly on v_z. Nonetheless, one can see the general nature of the result by considering the behavior of a single velocity group. For example, the Raman beat signal produced by the velocity group exactly resonant with the field after the excitation pulse is proportional to

$$|\tilde{c}_1(0)\tilde{c}_2^*(0)|^2\alpha_{13}\sin\alpha_{23}t\cos(\omega_{12}t+\phi)\,, \tag{18}$$

since $\delta_2=0$ and $g=(\delta_2^2+4\alpha_{23}^2)^{1/2}=2\alpha_{23}$ for these molecules. Expression (18) displays the essential features of our Raman beat experiments. Like all coherent Raman beats, the signal oscillates at $\omega_{12}t$ and its amplitude depends on having $c_1(0)c_2^*(0)$ nonzero after the excitation pulse. In addition, the signal is amplitude modulated at a frequency $\alpha_{23}=\wp_{23}E_0/2\hbar$. Note that this frequency is half the Rabi-flopping frequency $\wp_{23}E_0/\hbar$ (the frequency at which the population is driven back and forth between levels 2 and 3 by optical nutation). This behavior occurs because the Raman beat is produced by the term $\mathrm{Im}(\tilde{c}_1 c_3^*)$ in Eq. (12) and hence is proportional to the probability *amplitude* for being in a level, not the population in that level. (A transition being driven on resonance has probability amplitudes $c_u\propto\sin\alpha t$ and $c_l\propto\cos\alpha t$, with the optical nutation signal being proportional to $c_u c_l^*=\frac{1}{2}C\sin 2\alpha t$, C being some constant.) In an actual experiment one should not expect to see a Raman beat modulation that is just half the optical nutation frequency, however, because molecules which are not exactly on resonance have nutation and Raman beat modulation frequencies that differ from the resonant values [see Eq. (17)], and the actual signal is a sum over all detunings. Also, optical nutation signals from both the $3\rightarrow 1$ and $3\rightarrow 2$ transitions are present, and these have Rabi-flopping frequencies which differ by a factor of 4. As a result, appearance of the modulated Raman beat signal could be varied considerably by changing either

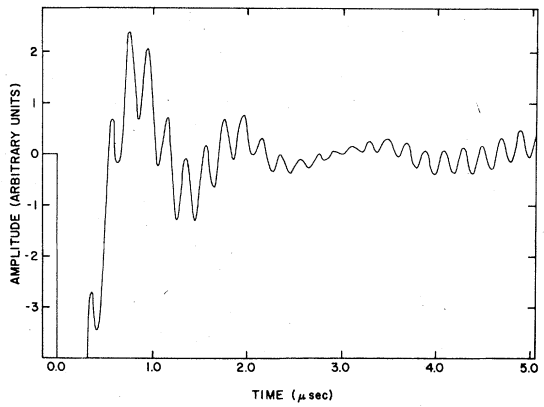

FIG. 4. Numerical solution of the three-level problem using parameters which approximate those of the upper trace in Fig. 3.

the Stark shift or the excitation pulse length. This point is discussed further in Sec. III.

Although we cannot expect our analytical calculations to be quantitatively correct, they do have the virtue of clearly showing the nature of the interaction between the one-photon optical nutation process and the two-photon Raman beat, i.e., optical nutation modulates the probability amplitude for level 2 and hence the amplitude of the Raman beat.

Exact calculations of the modulated Raman beat have also been made by numerically solving Eq. (6) for the c_i's followed by numerical integration of Eq. (12). Figure 4 shows a computer plot of such a calculation for $^{15}NH_3$ using a Stark pulse amplitude and width similar to that used in the upper trace of Fig. 3. The Raman signal is seen to go through a minimum at $t \simeq 3$ μsec as a result of the modulation. No attempt was made to fit the experiment quantitatively because of the extreme sensitivity of the result to the initial conditions (see Sec. III). There is, however, a good qualitative fit with the upper trace of Fig. 3.

Solving the probability amplitude equations rather than the density matrix equations means that we have no nontrivial steady-state solution. Thus our theory ignores the effects of the steady-state holes burned into both Doppler profiles before the excitation pulse. Not allowing for this steady-state hole in the population differences gives an anomalously large nutation signal background which must be subtracted out at the end of the calculation to give the curve of Fig. 4.

III. GENERAL FEATURES OF THE MODULATED RAMAN BEAT SIGNAL

The Raman beat signal obtained from numerical solutions was found to be an extremely sensitive function of the excitation pulse length and the frequency shift, and this sensitivity was also observed experimentally. The explanation for this behavior can be found by examining the distribution of excited velocity groups under the Doppler line profiles at the end of the excitation pulse as shown in Fig. 5. Initially the laser of frequency Ω lies somewhere within the Doppler profiles of the $3 \rightarrow 1$ and $3 \rightarrow 2$ transitions (see Fig. 1 for the level structure). The transition frequencies are shifted by an amount Δ for a time t_{ex} by the excitation pulse. As shown in the figure, this shifts the apparent laser frequency to a new position $\Omega + \Delta$ under the Doppler profiles. At the end of the excitation pulse the apparent laser frequency returns to Ω leaving a distribution of velocity groups excited as shown by the hatched areas in Fig. 5.[18] This excitation leads to a $\mathrm{sinc}(\omega t_{ex})$ frequency distribution for the probability amplitudes (i.e., the Fourier transform of a square pulse in time). The absolute value of this excited velocity distribution modulated by the Doppler profiles gives the excited distribution shapes shown in Fig. 5. The phases of the probability amplitudes are, of course, lost in this plot. The Raman signal is proportional to the product of the probability amplitudes and thus is related to the product of the depths of the excited velocity groups below the Doppler profiles shown in Fig. 5. Three representative velocity groups, A, B, and C, are indicated in the figure. Note that velocity group A will give a large Raman beat signal because both $|\tilde{c}_1|$ and $|\tilde{c}_2|$ are large, whereas group C will give a negligible Raman beat.

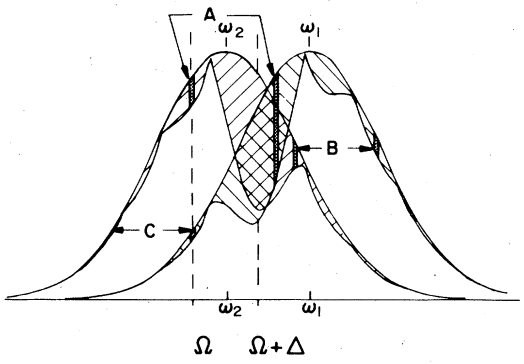

FIG. 5. Doppler profiles of the $3 \rightarrow 1$ and $3 \rightarrow 2$ transitions. For clarity, the level splitting and the frequency bandwidth of excited molecules have been greatly exaggerated. The hatched areas indicate the velocity groups which are excited by a rectangular Stark pulse. The laser frequency is Ω and its position with respect to the line centers ω_1 and ω_2 is shifted by an amount Δ during the Stark pulse. The amount of excitation for three different velocity groups A, B, and C are indicated by the heavily shaded vertical bars.

The fact that Raman beats are observed in a three-level system without degeneracy during the preparative stage is purely a consequence of using the short pulse to excite many molecular velocity groups to a coherent superposition of states. Had we not used a short excitation pulse the velocity group excited for one transition would not have significant excitation for the other transition and there would be no coherent Raman signal. In previous experiments the levels have been degenerate during the preparative stage and thus both transitions were always coherently excited.

The sensitivity of the beat signal amplitude to the excitation pulse width is caused by the changes in the side lobe positions of the sinc functions (outward for shorter pulses, inward for longer pulses). The number of coherently excited molecules goes through a series of maxima as the excitation pulse width is varied. By a similar argument, the number of velocity groups contributing to the Raman signal depends on the value of the frequency shift Δ during the pulse. Here again one would expect a series of Raman beat signal maxima as the frequency shift is varied.

The above dependences on the initial conditions imposed by the pulse (Stark voltage and duration) are observed experimentally as well as confirmed by numerical solutions to Eqs. (6). The numerical solutions also exhibit a power-dependent Raman beat frequency

$$\omega_{12}' = [\omega_{12}^2 + 4(\alpha_{13}^2 + \alpha_{23}^2)]^{1/2} . \tag{19}$$

This result is simply due to ac Stark shifts of the two transition frequencies. Brewer and Hahn have also calculated a power-dependent beat frequency which has the same form as our result except that decay was included in their calculation.[6,7] For the pressures used in our experiments the two results are essentially identical.

For couplings α_{ij} small compared to the level splitting ω_{12}, as in our experiments, $\omega_{12}' \simeq \omega_{12}$ and the nutation (which varies at the larger of the α_{ij}'s) is clearly distinguishable from the Raman beat signal. At the other extreme, if the couplings α_{ij} are comparable to or larger than the splitting, the clear observation of a Raman beat becomes very difficult. The Raman beat frequency is then nearly equal to the nutation frequency, and the distinction between the Raman beat and nutation is obscured. This explains why Raman beats have not been observed in molecules such as NH_2D where we have also studied three-level systems.[19-21] There, the excited-state splittings are comparable to the nutation frequencies, and reducing the power enough to make the nutation slower than the Raman beat results in a signal too small to observe.

IV. EXPERIMENTAL RESULTS

An understanding of the Raman beat behavior discussed above allows one to accurately determine molecular constants from the Raman signal. In particular, the Raman beat frequency ω_{12} determines the excited-state dipole moment for the $^{15}NH_3$ transition studied, and the decay of the Raman beat signal as a function of $^{15}NH_3$ gas pressure determines the Raman decay rate.

The average of the observed Raman beat frequency from nine experimental runs was $\omega_{12}' = 5.28 \pm 0.02$ MHz, and, the nutation frequency was ~0.3 MHz. This gives a power corrected excited-state frequency splitting of $\omega_{12} = 5.27 \pm 0.03$ MHz. From Shimizu's measurements for the molecular constants[10] of $^{15}NH_3$ and the value of ω_{12}, taking into account all Stark effects from neighboring levels, we calculate the excited-state permanent electric dipole moment to be

$$\mu_{ex} = 1.286 \pm 0.010 \text{ D} .$$

This compares with Shimizu's calculated value of 1.26 ± 0.02 D obtained from Stark splittings of widely separated spectral lines.[10]

The Raman decay rate Γ_r can be calculated directly from the pressure dependence of the Raman beat decay as long as the Raman beat modulation discussed in Sec. III can be neglected. A total power of ~0.08 W with a peak intensity of <2 W/cm^2 was used in these experiments giving a nutation frequency and thus a Raman beat modulation frequency slow compared to the signal decay rates. If any small residual modulation is still present, its effect should be independent of pressure and would only change the intercept of a plot of decay rate versus pressure. Making such a plot for runs at seven different pressures yields a straight line whose slope is the Raman decay rate for the $(\nu_2, J, K) = (0^a, 2, 2) \rightarrow (1^s, 3, 2)$ transition. We find

$$\Gamma_r = 63 \pm 6 \text{ MHz/Torr} .$$

Only the excited-state decays are involved in the two-photon Raman process and our result agrees with the excited-state population decay rate of 66 ±6 MHz/Torr which we have measured using delayed optical nutation.[20] This agreement shows, as has been found for other infrared transitions, that phase-changing collisions are negligible. In general we would not expect to see phase-changing collisions in an infrared transition since the dipole oscillates at $\sim 5 \times 10^{13}$ Hz, while a collision typically lasts about 10^{-12} sec. Therefore only about 50 cycles of the dipole oscillation occur during the collision, and, in order to change the dipole phase appreciably, the resonant frequency will need to

be shifted by about 1%, or $\sim 5 \times 10^{11}$ Hz. This shift is considerably larger than most rotational energy-level spacings so that any collision producing such a large shift will almost certainly change the rotational state. As a result, phase-changing collisions are not observed in molecules even when one might expect to see them on the grounds that the upper and lower states are affected differently during the collision, as they are in $^{15}NH_3$.[22]

ACKNOWLEDGMENTS

This work supported in part by the National Science Foundation and in part by the Air Force Office of Scientific Research and Army Research Office. E. V. S. also gratefully acknowledges support by the North Texas State University Faculty Research Fund, and R. L. S. acknowledges support by the Alfred P. Sloan Foundation.

[1]R. L. Shoemaker and R. G. Brewer, Phys. Rev. Lett. 28, 1430 (1972).
[2]M. M. T. Loy, Phys. Rev. Lett. 36, 1454 (1976).
[3]P. F. Liao, J. E. Bjorkholm, and J. P. Gordon, Phys. Rev. Lett. 39, 15 (1977).
[4]M. M. T. Loy, Phys. Rev. Lett. 39, 187 (1977).
[5]F. A. Hopf, R. F. Shea, and M. O. Scully, Phys. Rev. A 7, 2105 (1973).
[6]R. G. Brewer and E. L. Hahn, Phys. Rev. A 8, 464 (1973); 9, 1497E (1973).
[7]R. G. Brewer and E. L. Hahn, Phys. Rev. A 11, 1641 (1975).
[8]J. R. R. Leite, R. L. Sheffield, M. Ducloy, R. D. Sharma, and M. S. Feld, Phys. Rev. A 14, 1151 (1976).
[9]P. R. Berman, J. M. Levy, and R. G. Brewer, Phys. Rev. A 11, 1668 (1975).
[10]F. Shimizu, J. Chem. Phys. 53, 1149 (1970).
[11]C. Freed, IEEE J. Quantum Electron. 4, 404 (1968); 3, 203 (1967).
[12]R. L. Shoemaker, in *Laser and Coherence Spectroscopy*, edited by J. I. Steinfeld (Plenum, New York, 1978), pp. 197–371.
[13]G. B. Hocker and C. L. Tang, Phys. Rev. Lett. 21, 591 (1968).
[14]A. Javan, Phys. Rev. 107, 1579 (1957).
[15]M. Sargent III and P. Horwitz, Phys. Rev. A 13, 1962 (1976).
[16]A. Schenzle and R. G. Brewer, Phys. Rep. 43, 455 (1978).
[17]R. G. Brewer and R. L. Shoemaker, Phys. Rev. A 6, 2001 (1972).
[18]Note that the steady-state hole burned into the lines before the excitation pulse is neglected in Fig. 5 and in the theoretical result of Eq. (18).
[19]R. L. Shoemaker and F. A. Hopf, Phys. Rev. Lett. 33, 1527 (1974).
[20]E. W. Van Stryland, Ph.D. thesis (University of Arizona, 1976) (unpublished).
[21]R. L. Shoemaker and E. W. Van Stryland, J. Chem. Phys. 64, 1733 (1976).
[22]M. M. T. Loy, Phys. Rev. Lett. 32, 814 (1974).